INTERNATIONAL JOURNAL OF PRECISION ENGINEERING AND MANUFACTURING Vol. 19, No. 4, pp. 577-586 APRIL 2018 / 577

REGULAR PAPER

DOI: 10.1007/s12541-018-0070-7
ISSN 2234-7593 (Print) / 2005-4602 (Online)

Determination of Optimal Riding Positions using Muscle Co-Contraction on Upper Extremity during Manual Standing Wheelchair Propulsion

Jeseong Ryu[1], Jongsang Son[2,3], Sungjoong Kim[1], Jongman Kim[1], Soonjae Ahn[1], and Youngho Kim[1,#]

1 Department of Biomedical Engineering, Yonsei University, 1, Yeonsedae-gil, Heungeop-myeon, Wonju-si, Gangwon-do, 26493, Republic of Korea
2 Sensory Motor Performance Program, Rehabilitation Institute of Chicago, Chicago, IL 60611, USA
3 Department of Physical Medicine & Rehabilitation, Northwestern University, Chicago, IL 60611, USA
Corresponding Author / E-mail: younghokim@yonsei.ac.kr, TEL: +82-33-760-2492
ORCID: 0000-0001-7531-802X

KEYWORDS: Standing wheelchair, Optimal riding position, Muscle activation, Integrated electromyography, Wheelchair dynamometer

A newly designed standing wheelchair that moves even while standing posture has been developed to improve the health and the quality of life for wheelchair users. However, this standing wheelchair has hand rims separate from the wheels, likely affecting the biomechanical characteristics and the efficiency of propulsion. Thus, this study aimed to propose a method to determine the optimal riding position by evaluating muscle activation during manual standing wheelchair propulsion. Ten elderly male subjects were asked to propel the hand rims with nine different seat (while sitting) and footrest (while standing) positions. During the experiments, kinematic data were obtained using a 3D motion capture system and sEMG measurement system, respectively. Simultaneously, surface electromyography signals were recorded from eleven muscles on the right side of the trunk and the upper extremity to evaluate relative iEMG and muscle co-contraction ratio. The muscle co-contraction ratio was higher at positions (upward and backward directions) distant from the hand rim and lower at positions (downward and forward directions) close to the hand rim. These results indicate that decreased distance from the hand rim enhances joint stability and decreases muscle co-contraction. These results also showed a good similarity with our previous study using energy expenditure method.

Manuscript received: July 19, 2017 / Revised: December 15, 2017 / Accepted: January 9, 2018

1. Introduction

Wheelchair is the most familiar and the important mobile device for individuals with the loss of mobility. In all wheelchair users, the proportion of elderly people over 65 was 56% and 96% of them used manual wheelchairs.[1] Although electric powered wheelchairs are more convenient, manual wheelchairs are prescribed for most people with disabilities except those with conditions such as obesity, overuse of the upper limbs, long-time living with a disability, and poor health and nutrition because manual wheelchairs are easy to use and affordable and maintain upper body strength and endurance. Despite the advantage and the necessity of manual wheelchairs, its long-term use is associated with various upper extremity injuries.[2] Therefore, many previous studies have evaluated the effects of seat position or propulsion pattern on physiological and biomechanical outcomes since many researchers considered that overuse of the arm in an inefficient way may be related to pain and injury.[3-6]

According to previous studies regarding changes in the propulsion pattern and muscle activity depending on different seat positions, Masse et al.[7] investigated that the relationship between the seat position and muscle activation. They measured the kinematics and surface electromyography (sEMG) from shoulder muscles for five male paraplegics in six different seat positions. As a result, they concluded the backward-low and the middle-low position were the most efficient position because the overall integrated EMG (iEMG) and pushing frequency were lower than other position. Louis et al.[8] measured upper limb muscle activation and kinematics during wheelchair propulsion in twelve different seat and axle positions with ten able-bodied and ten paraplegic subjects. They divided the push phase in two parts for a more precise analysis and found no significant difference for push percentage over cycle propulsion between the paraplegic group and the able-bodied group, but early push time was significantly longer for the

paraplegic group than for the able-bodied group. Also, they found that muscle activation was increased for lower seat positions during push phases.

The increase in muscle activation does not only contribute to an increase in propulsion force, but also contributes to the stability of the propulsion operation. In the other study, muscle co-contraction improved the motion accuracy.[9] They assumed that although energetically expensive, co-contraction might be a strategy used by the motor system to facilitate multi-joint arm movement accuracy. In addition, co-activation of antagonist muscles is readily observed early in motor learning, in interactions with unstable mechanical environments and in motor system pathologies.[10] According to the elderly studies, the co-contraction of the antagonist muscle for the elderly are frequently found than that of the young one.[11] Son et al.[12] applied co-contraction of the antagonist muscle and showed that co-contraction ratio (CR) of the elderly decreased significantly in 4 weeks after upper arm elbow robotic rehabilitation training. Therefore, evaluation of iEMG and co-contraction of antagonist muscles are very important to determine the efficiency and appropriateness of wheelchair propulsion.

Wheelchair standing devices is highly recommended to long-term wheelchair users for improvement of their health problem,[13,14] though most of them cannot move in a standing posture because they have similar hand rim and wheel structure like the traditional wheelchair. Recently, a newly designed standing wheelchair has been developed to move even while standing. Unlike the traditional wheelchair standing devices, the manual standing wheelchair has hand rims separate from the wheels, likely affecting the biomechanical characteristics of propulsion. Considering that most wheelchair users are the elderly patient as a result of sudden onset of disability (e.g., SCI, stroke), gradual onset of progressive diseases (e.g., osteoarthritis, multiple sclerosis), or loss of walking mobility,[15,16] investigations regarding the position of the hand rim with respect to the user on the propulsion efficiency should be conducted to suggest an optimal riding position of the manual standing wheelchair.

In this study, muscle activations of the upper-limb joints at nine different positions were evaluated to determine an optimal position of the hand rims with respect to the user during manual propulsion and sitting/standing in the manual standing wheelchair. During the manual propulsion, the upper-limb kinematics and muscle activations were measured, thereby calculating iEMG and co-contraction of antagonist muscles. The hypothesis of this study was that the optimal riding position would have the smallest co-contraction of antagonist muscles during manual propulsion in sitting and standing postures.

2. Methods

2.1 Experiment apparatus

Our brake-type dynamometer has been developed to measure the torques and RPMs during the propulsion of various wheelchairs.[3] It consists of two dynamometers for each wheel and two support frames for the front and rear casters. Each dynamometer has a roller (Φ200 × 400 mm, steel tubular), torque sensor (TMA-2KM, Setech Co., Ltd., KR) with an RPM sensor (MP-981, Setech Co., Ltd., KR), and powder brake (PRB-1.2Y3, Pora electric machinery Co., Ltd., KR) connected in series, using shafts and bearings. Thus, it can measure both roller-axis torque and RPMs generated by a wheel during the propulsion. Finally, these can be used to determine the wheel-axis torque, RPM, and propulsion tangential force.

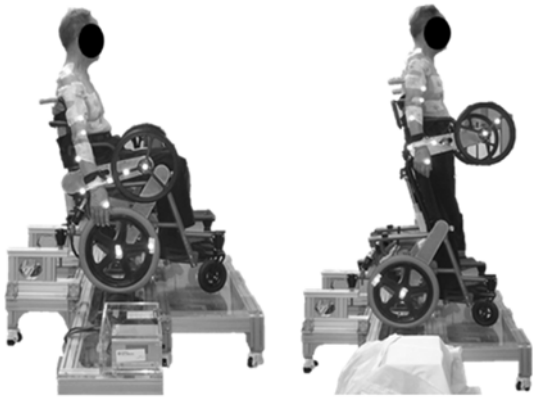

Fig. 1 Experimental setup for the standing wheelchair prototype installed on the brake-type dynamometer

The powder brake can control the roller-axis rolling resistance by the voltage control knob. The minimum rolling resistance is 0 N·m at 0 V, and the maximum is 17 N·m at 24 V. In this study, the rolling resistance was set at 0.55 N·m (at 3 V) because such setting best simulated the laboratory floor (carpet) condition.

A prototype of the manual standing wheelchair (HANIL Hightech Co., Ltd., KR) was installed on the dynamometer system (Fig. 1). The manual standing wheelchair has two hand rims separated from each wheel enabling their use in the standing position as well. The diameters of the hand rim and wheel were 320 and 380 mm, respectively. The seat was 380 mm wide and 400 mm deep. The seat's backrest was 35.3 cm behind and 3.2 cm below the hand rim center. The footrest was 92 cm below the hand rim center. The initial positions of the seat and footrest were defined as the original positions (middle-center). The dimensions of the standing wheelchair were determined by the manufacturer according to the anthropometric data of normal adults.

2.2 Experiment procedure

Ten elderly male subjects, who showed no sign of injury or pathological diagnosis on their upper body, participated in this study (Table 1). Prior to the experiment, all participants provided informed written consent, which was approved by the Institutional Review Board of Yonsei University (No. 1041849-201406-BM-029-01). Subject groups had significant difference in height only. Seven spherical reflective markers (14 mm in diameter) were attached to the subjects' right upper limb according to the Plug-In-Gait model (Oxford Metrics Ltd., UK). Two additional markers were positioned at the rotation center of the hand rim and the middle of the hand rim spoke to directly measure the propulsion angles of the hand rim. Also, surface electromyography (sEMG) signals were collected using an EMG measurement system (Trigno^{TM} wireless systems, Delsys Inc., USA). Eleven wireless electrodes were attached on the right side of the trunk and the upper extremity. The subjects were asked to sit on the standing wheelchair, leaning back on the backrest and to familiarize themselves with the

Table 1 Subject characteristics (mean ± SD)

Characteristics	Short group N=5	Tall group N=5	*p*-value*
Age (yr)	76.4 ± 1.9	75.4 ± 2.9	0.538
Mass (kg)	55.9 ± 10.2	66.0 ± 9.1	0.138
Height (cm)	160.2 ± 2.9	166.6 ± 1.6	0.003

*Unpaired *t*-test, significant difference between groups ($p < 0.05$)

Table 2 Muscle names and their abbreviations

Muscle name	Abbreviation
Deltoid Anterior	DA
Pectoralis Major	PM
Biceps Brachii	BB
Serratus Anterior	SA
Forearm Flexor	FF
Trapezius Descendens	TD
Trapezius Transversus	TT
Deltoid Posterior	DP
Infraspinatus	IS
Triceps Brachii	TB
Forearm Extensor	FE

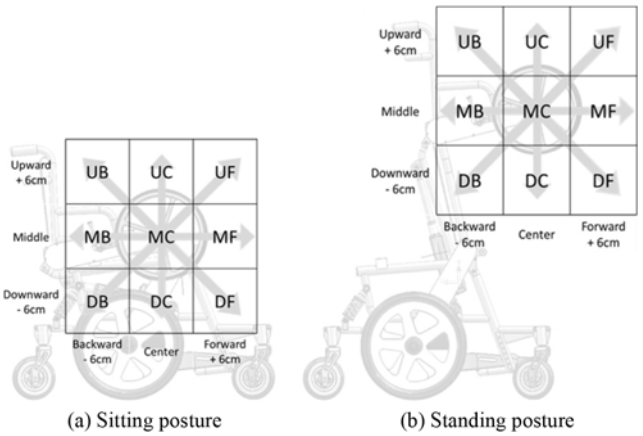

Fig. 2 Distance between the hand and hand rim: Nine positions in the sitting and standing posture

propulsion of the standing wheelchair for 2-3 minutes. Thereafter, they were instructed to propel the hand rims with different seat and footrest positions at their self-selected speed.

To determine the relative position of the hand rim, nine different positions were chosen as follows: the neutral position (middle-center, MC); 6 cm forward from MC (middle-forward, MF); 6 cm backward from MC (middle-backward, MB); 6 cm upward from MC (up-center, UC); 6 cm forward from UC (up-forward, UF); 6 cm backward from UC (up-backward, UB); 6 cm downward from MC (down-center, DC); 6 cm forward from DC (down-forward, DF); and 6 cm backward from DC (down-backward, DB) as shown in Fig. 2. The subjects propelled ten consecutive cycles for each position assigned randomly. Kotajarvi et al.[18] reported no significant difference in wheelchair propulsion among different hand-rim positions distant 3.3-4 cm apart. Therefore, the distance of different ride positions was set by 6cm apart in this study.

During the experiments, the marker trajectories were recorded at 200 Hz, using a 3D motion capture system (Vicon MX system, Vicon Motion System Ltd., UK). In addition, the analog data measured from the dynamometer were simultaneously obtained at 1 kHz, using an analog sync box (Vicon MX system, Vicon Motion System Ltd., UK). All raw sEMG signals from each muscle were simultaneously recorded at a sampling rate 1 kHz (bandpass filtered from 5 to 450 Hz using a 4th order Butterworth filter) and low pass filtered with a cutoff frequency of 4 Hz using a 4th order Butterworth filter to eliminate ambient noise and smoothen the curve.

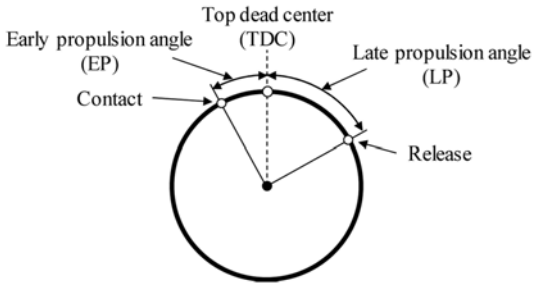

Fig. 3 Definition of a propulsion cycle

2.3 Data analysis

The kinematic and sEMG data were exported to MATLAB software (MathWorks Inc., MA, USA) for analysis and post-processing. Three different phases were defined in a propulsion cycle: the early push phase (EP), the late push phase (LP), and the recovery phase (RP). EP began from hand rim contact and finished before the hand passed the top dead center (TDC) of the hand rim. LP began when the hand passed the TDC and finished when the hand released the hand rim. RP was defined as from releasing the hand rim to next gripping the hand rim.[8]

Propulsion angles of two push phases were determined using the trajectory of two reflective markers attached on the hand rim. Mean propulsion angle data were calculated from six propulsion cycles, excluded for the first two and the last two cycles among ten propulsion cycles. As shown in our previous study, the propulsion angle depends on the riding position and directly affects the propulsion efficiency.[3] Therefore, the mean propulsion angle was normalized by the one at the neutral position (MC).

$$PAR = \frac{PA}{PA_{MC}} \times 100(\%) \tag{1}$$

where *PAR* indicates the propulsion angle ratio and *PA* and PA_{MC} indicate the propulsion angle at each position and MC position, respectively.

Integrated EMG (iEMG) on each phase was determined by integrating sEMG signal.

$$iEMG_{Each\ phase} = \int_{t_1}^{t_2} sEMG\,dt \tag{2}$$

where t_1 represents the onset, t_2 the offset, and *dt* the time interval (i.e., 0.001 s).

Thereafter iEMG values for all positions were normalized to the one in MC position to compare a relative muscle activation among different nine riding positions. In addition, iEMG value were also normalized to *PAR* of each position to compare a relative muscle activation per equivalent propulsion angle.

$$iEMG_{Normal} = \frac{iEMG}{iEMG_{MC} \times PAR} \quad (3)$$

To compare iEMG between groups, mean iEMGs were calculated for subject groups and the co-contraction ratio (CR) was also calculated within the groups.

$$CR = \frac{\Sigma iEMG_{Antago}}{\Sigma(iEMG_{Ago} + iEMG_{Antago})} \times 100(\%) \quad (4)$$

where $iEMG_{Ago}$ is the iEMG of the agonist muscles and, $iEMG_{Antago}$ is the iEMG of the antagonist muscles.

2.4 Statistical analysis

All statistical analyses were performed using the IBM SPSS Statistics (Version 22, IBM Corp., USA). Repeated measures analysis of variance was applied with the position of the hand rim as the main factor to detect significant differences in the biomechanical variables. An unpaired t-test was performed to compare the subject groups' characteristics. Based on a significant level of $p<0.05$, post hoc analyses were conducted and corrected for multiple comparisons using LSD tests. Greenhouse-Geisser and Huynh-Feldt corrections were performed for the sphericity of statistical analysis.

3. Results

3.1 Propulsion angle

Figs. 4 and 5 show the propulsion angle for EP, LP, RP in various positions for short and tall subject groups. In sitting posture, for the short group, the propulsion angle became minimal (44.0±9.8°) in UF position and the maximal (56.0±10.2°) in UB position in EP. On the other hand, the smallest propulsion angle during LP was 51.8±6.1° in UB position and the largest was 93.2±7.3° in DF position. As a result, the propulsion angle was the smallest (100.8±14.5°) in UC position and the largest (140.3±17.3°) in DF position in the total push phase. For the tall group, the propulsion angle became minimal (29.8±8.3°) in DF position and the maximal (47.5±8.5°) in MB position in EP. On the other hand, the smallest propulsion angle during LP was 52.0±13.0° in UB position and the largest was 93.9±13.2° in DF position. As a result, the propulsion angle was the smallest (96.8±19.8°) in UB position and the largest (125.4±23.6°) in DC position in the total push phase. In standing posture, for the short group, the propulsion angle became minimal (48.0±16.3°) in UF position and the maximal (57.6±15.2°) in UB position in EP. On the other hand, the smallest propulsion angle during LP was 56.6±11.0° in UB position and the largest was 91.9± 13.8° in DF position. As a result, the propulsion angle was the smallest (114.2±17.8°) in UB position and the largest (140.2±24.8°) in DF position in the total push phase. For the tall group, the propulsion angle became minimal (42.1±10.3°) in MF position and the maximal (57.6± 13.3°) in MB position in EP. On the other hand, the smallest propulsion angle during LP was 55.0±10.6° in UB position and the largest was 91.7±26.3° in DF position. As a result, the propulsion angle was the smallest (108.6±19.8°) in UB position and the largest (135.8±38.5°) in DF position in the total push phase.

The short subject group showed a significantly larger propulsion

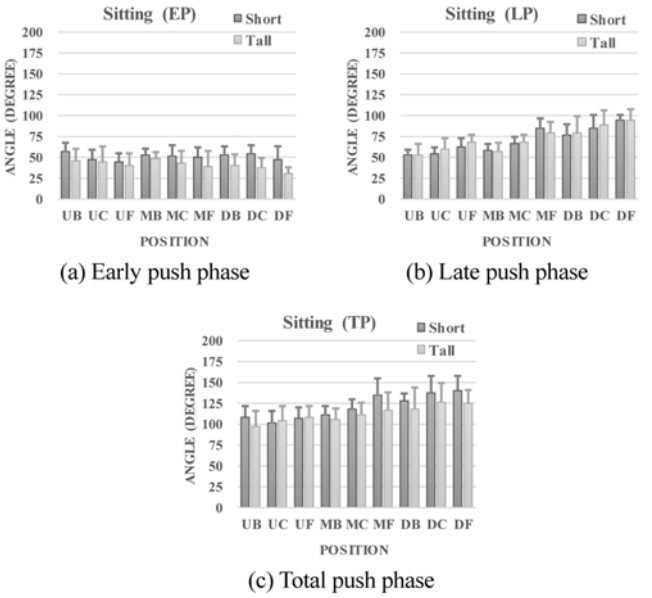

Fig. 4 Propulsion angle at various positions in sitting posture for short and tall subject groups

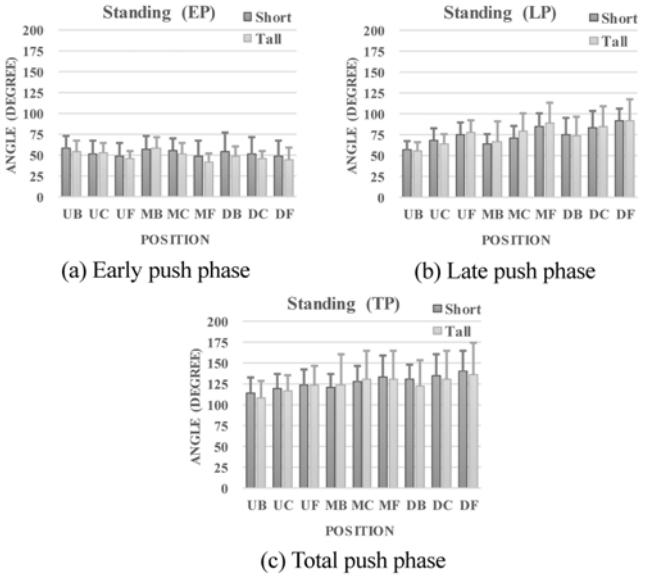

Fig. 5 Propulsion angle at various positions in standing posture for short and tall subject groups

angles than the tall subject group in EP for sitting and standing posture ($p<0.05$). The propulsion angles in downward positions were also significantly larger than the ones in upward positions during total push phase in sitting and during LP and total push phases in standing postures ($p<0.05$). Propulsion angles in forward positions were also significantly larger than the ones in backward positions during total push phase in sitting and during LP in standing postures ($p<0.05$).

3.2 Propulsion time

Figs. 6 and 7 show the propulsion time for EP, LP, RP in various positions for short and tall subject groups.

In the short group, EP was longer than LP in all positions for the

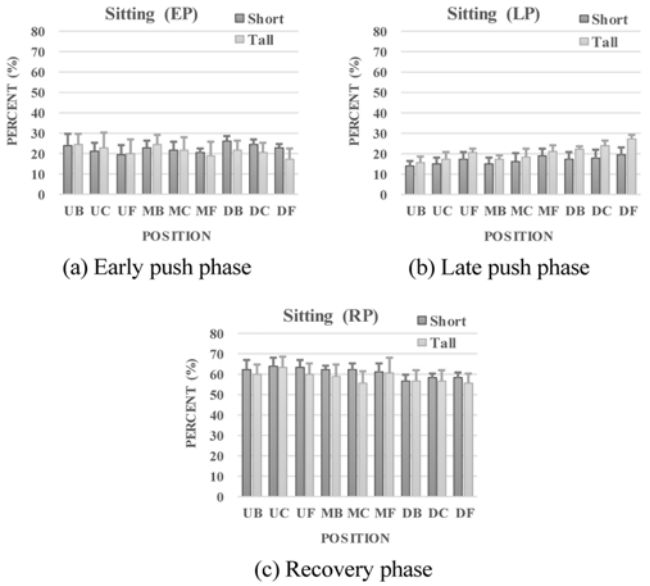

Fig. 6 Cycle percentage at various positions in sitting posture for short and tall subject groups

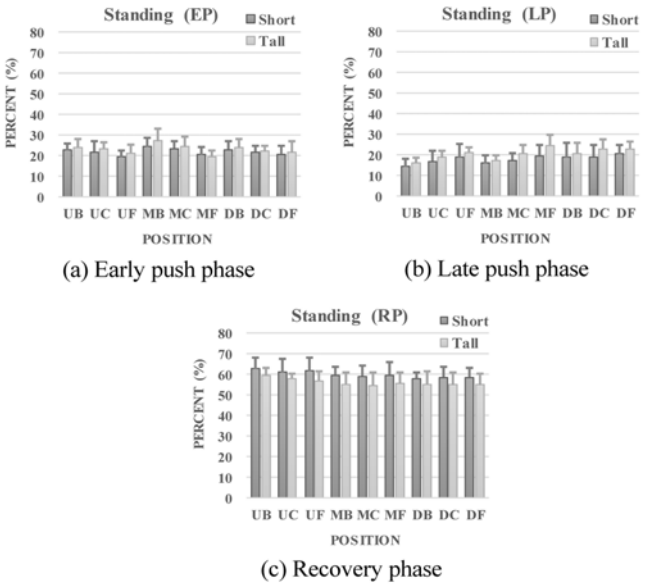

Fig. 7 Cycle percentage at various positions in standing posture for short and tall subject groups

Table 3 Propulsion time (mean ± SD, %cycle)

Phase		Early push time (ET)		Late push time (LT)		Recovery time (RT)	
Posture		Avg.	S.D.	Avg.	S.D.	Avg.	S.D.
Sit	Short	22.5	2.1	16.6	1.8	60.9	2.6
	Tall	21.1	2.3	20.2	3.6	58.7	2.1
Stand	Short	22.1	1.5	18.0	2.0	59.9	1.6
	Tall	23.1	2.1	20.8	2.8	56.1	1.7

both sitting and standing postures. However, for sitting posture, LP in downward position was longer than EP in the tall subject group. Regardless of the subject groups and riding postures, EP time became gradually decreased from the backward to the forward positions, whereas LP time became gradually increased from the backward to the forward positions. Mean time was 22.2%, 18.9%, and 58.9% for EP, LP, RP, respectively (Table 3).

However, the statistical analysis showed no significant differences between groups in all conditions. In sitting posture, EP time in middle and downward positions showed significantly longer time in backward position than the ones in forward position (p<0.05). There were some significant differences between positions, but no trends were found in standing posture. LP time in DF position showed significantly longer than the ones in all other positions in sitting position (p<0.05).

In standing posture, LP time in UB position showed significantly shorter time than the ones in all other positions except the one in MB position (p<0.05). Also, LP time in upward and middle positions showed significantly shorter time in backward position than the ones in forward position (p<0.05). RP time in upward positions showed significantly longer time than the ones in downward positions in sitting posture (p< 0.05) and RP time in UB position was significantly longer than the ones in all other positions except the one in UF position (p<0.05).

3.3 Normalized iEMG

Table 4 and 5 show the normalized muscle activation by the value at MC position during EP for short and tall subject group. In sitting posture, relatively large muscle activations were observed in TD and TT muscles at DF position for short subject group and DA, BB, TD, DP, TB, and FE muscles at DB position for tall subject group. In standing posture, SA and TB muscles showed relatively large muscle activations in DB position for short subject group and DA, SA, DP, TB, and FE muscles showed relatively large muscle activations in DB position. In addition, DA, BB, SA, IS, and TB muscles showed larger muscle activations in backward positions than in forward positions in both sitting and standing postures.

Table 6 and 7 show the normalized muscle activation by the value at MC position during LP for short and tall subject group. In sitting posture, relatively large muscle activation was observed in TD muscle at DC and DF position for short subject group. For tall subject group, relatively large muscle activations were observed in DA, SA, IS, TB, and FE muscles at UB position. TD muscle showed relatively large muscle activation in downward positions. On the other hand, in standing posture, SA and TB muscles showed relatively large muscle activations in DB position for short subject group. Also, IS and TB muscles showed relatively large muscle activations in backward positions than forward positions in standing postures. For tall subject group, IS muscle showed drastically large muscle activation in DF position. DA, SA, and IS muscles also showed relatively large muscle activations in backward positions than forward positions in both sitting and standing postures.

Table 4 Normalized iEMG in sitting during early push phase (%iEMG at MC position)

(a) Short subjects

Position	DA	PM	BB	SA	FF	TD	TT	DP	IS	TB	FE
UB	103.8	68.5	116.1	119.6	93.6	80.4	88.7	98.4	125.9	74.5	100.9
UC	112.0	112.5	100.0	119.4	125.2	84.6	110.1	111.6	123.2	104.9	122.5
UF	106.7	112.2	89.8	108.0	119.5	88.9	111.5	103.0	115.9	86.5	119.9
MB	102.5	91.9	97.0	102.9	111.8	85.6	102.1	96.0	118.2	104.0	90.4
MC	100.0	100.0	100.0	100.0	100.0	100.0	100.0	100.0	100.0	100.0	100.0
MF	111.5	112.6	100.9	100.8	96.1	125.0	124.0	84.1	101.7	78.6	103.1
DB	119.3	113.0	107.6	103.9	104.1	141.6	94.1	193.2	115.3	131.0	117.8
DC	125.6	124.3	101.6	91.4	114.4	178.6	106.7	146.4	94.6	122.7	98.5
DF	140.6	152.9	129.6	104.7	122.1	238.1	191.3	174.2	87.3	132.6	99.0

(b) Tall subjects

Position	DA	PM	BB	SA	FF	TD	TT	DP	IS	TB	FE
UB	109.0	76.5	115.9	125.6	80.9	102.3	110.0	112.3	148.0	92.9	106.5
UC	105.6	122.9	114.6	102.0	86.3	87.6	110.7	97.4	126.1	88.4	115.2
UF	96.3	104.2	99.4	83.1	78.2	84.5	124.8	106.4	94.2	75.9	119.2
MB	105.5	85.2	114.4	132.7	95.1	99.8	89.6	103.5	134.2	105.3	110.8
MC	100.0	100.0	100.0	100.0	100.0	100.0	100.0	100.0	100.0	100.0	100.0
MF	95.4	118.2	109.7	87.3	88.3	99.1	121.8	119.0	79.5	94.7	119.0
DB	117.9	103.7	134.7	104.1	108.4	136.5	108.8	156.4	123.4	165.0	129.6
DC	97.7	117.0	117.4	91.5	113.6	127.1	98.2	131.2	79.7	153.4	122.2
DF	74.0	111.5	97.0	80.0	91.1	128.7	88.3	124.6	57.1	133.1	101.7

Table 5 Normalized iEMG in standing during early push phase (%iEMG at MC position)

(a) Short subjects

Position	DA	PM	BB	SA	FF	TD	TT	DP	IS	TB	FE
UB	102.1	74.9	96.2	101.7	89.7	69.6	93.1	96.1	118.1	106.1	104.0
UC	106.3	107.7	89.0	100.9	112.4	75.5	122.3	96.7	98.6	109.0	104.8
UF	100.8	121.2	85.5	101.3	105.7	84.5	129.2	104.4	81.1	95.2	97.1
MB	100.4	82.8	80.7	117.0	103.4	74.0	85.4	112.3	109.9	122.0	108.9
MC	100.0	100.0	100.0	100.0	100.0	100.0	100.0	100.0	100.0	100.0	100.0
MF	102.0	117.2	97.9	103.5	99.8	101.5	118.0	132.9	84.2	97.9	94.0
DB	107.3	100.7	82.1	207.3	97.7	80.6	80.8	138.7	122.1	210.2	124.1
DC	100.8	120.0	101.1	134.4	104.9	112.8	106.4	145.8	103.5	172.1	112.8
DF	100.1	130.6	99.6	133.2	114.7	123.4	120.1	157.2	84.5	139.7	94.2

(b) Tall subjects

Position	DA	PM	BB	SA	FF	TD	TT	DP	IS	TB	FE
UB	106.6	90.8	102.7	115.5	95.4	82.7	84.0	82.2	128.0	110.8	76.7
UC	95.6	107.2	104.8	95.0	85.8	70.5	82.0	72.6	90.3	93.1	94.9
UF	90.3	111.8	80.4	94.1	110.2	79.4	83.7	82.2	80.1	83.0	81.2
MB	112.3	81.9	122.1	127.6	106.4	98.5	90.6	88.3	146.3	107.2	125.5
MC	100.0	100.0	100.0	100.0	100.0	100.0	100.0	100.0	100.0	100.0	100.0
MF	87.3	107.1	86.8	108.7	98.2	94.2	82.4	74.1	69.5	88.8	69.7
DB	121.3	81.3	113.4	142.5	107.8	120.2	70.8	106.3	118.7	137.2	139.8
DC	108.4	108.6	102.7	115.2	105.1	123.3	93.7	100.5	97.9	136.6	88.3
DF	109.4	123.4	93.7	115.0	115.6	123.1	98.4	79.8	76.4	116.9	85.6

3.4 Co-contraction ratio of normalized iEMG

Muscle co-contraction ratio (CR) was different depending on subject groups and propulsion phases in sitting posture (Fig. 8). During EP, CR of the short group was the smallest (96%) at DC position and the largest (104%) at UB and DB positions. On the other hand, the tall group showed the smallest CR (98%) at DF position and the largest(106%) at UB position. It is noted that both groups tended to show decreased CR as moving forward or downward from MC position. During LP, CR of the short group was the smallest (85%) at DC position and the largest (104%) at MB position. The tall group showed the smallest CR (91%) at DF position and the largest (105%) at MF position. It is interesting that both groups showed larger CR at middle positions and smaller CR at downward positions.

In standing posture (Fig. 9), during EP, CR of the short group was the smallest (98%) at DB position and the largest (105%) at UB position. On the other hand, the tall group showed the smallest CR (90%) at DF position and the largest (101%) at MB position. It is noted that both groups tended to show decreased CR as moving forward or downward from MC position. During LP, CR of the short group was the smallest (92%) at DF position and the largest (108%) at UB position. The tall

Table 6 Normalized iEMG in sitting during late push phase (%iEMG at MC position)

(a) Short subjects

Position	DA	PM	BB	SA	FF	TD	TT	DP	IS	TB	FE
UB	108.7	73.7	108.1	129.7	114.1	111.8	100.4	115.9	131.3	102.4	98.5
UC	99.4	106.9	118.5	130.5	127.9	115.8	136.2	114.7	110.2	113.7	120.1
UF	103.0	114.4	117.8	132.3	142.3	167.0	143.2	115.0	99.9	113.9	107.6
MB	97.0	86.4	101.5	95.3	93.3	92.6	109.3	94.1	124.2	91.3	93.6
MC	100.0	100.0	100.0	100.0	100.0	100.0	100.0	100.0	100.0	100.0	100.0
MF	89.3	108.6	97.3	109.3	111.8	118.7	129.2	103.2	69.3	98.2	81.6
DB	91.3	79.8	116.0	70.7	76.9	134.8	93.7	94.4	75.4	80.8	87.8
DC	93.5	99.3	90.5	68.1	93.6	240.4	111.2	75.6	61.7	72.2	71.2
DF	91.7	131.5	90.0	71.6	95.9	184.7	122.3	83.6	58.9	69.0	73.7

(b) Tall subjects

Position	DA	PM	BB	SA	FF	TD	TT	DP	IS	TB	FE
UB	154.2	87.5	100.3	130.0	107.1	115.5	95.0	127.0	152.2	108.1	133.3
UC	108.6	112.3	101.9	108.4	106.3	89.2	76.5	110.6	112.4	100.0	126.6
UF	112.5	116.3	106.9	101.0	103.2	89.4	86.0	114.0	93.9	97.1	99.2
MB	121.5	88.0	88.0	124.6	110.4	106.8	79.2	96.9	117.8	101.6	95.9
MC	100.0	100.0	100.0	100.0	100.0	100.0	100.0	100.0	100.0	100.0	100.0
MF	91.3	106.2	99.7	91.9	95.1	103.6	150.3	104.1	91.5	99.5	97.1
DB	111.6	65.7	105.5	94.0	112.0	164.6	94.1	111.4	134.2	77.5	89.0
DC	91.0	80.7	93.7	78.2	132.3	136.1	94.1	99.0	99.1	99.1	82.0
DF	81.7	102.4	87.8	75.9	96.6	199.9	100.2	91.3	79.8	85.2	78.6

Table 7 Normalized iEMG in standing during late push phase (%iEMG at MC position)

(a) Short subjects

Position	DA	PM	BB	SA	FF	TD	TT	DP	IS	TB	FE
UB	113.3	79.1	102.4	110.6	95.2	66.4	97.0	135.2	122.0	121.7	100.2
UC	105.0	97.8	98.0	101.4	100.9	72.4	96.1	93.9	108.4	102.3	89.0
UF	109.6	128.0	109.7	113.6	95.0	76.8	82.6	91.8	89.8	116.1	91.7
MB	100.7	80.0	99.4	104.1	95.6	72.6	97.5	115.3	112.9	137.4	99.0
MC	100.0	100.0	100.0	100.0	100.0	100.0	100.0	100.0	100.0	100.0	100.0
MF	113.2	119.1	98.9	102.7	86.7	111.7	94.9	94.4	88.6	111.6	98.2
DB	94.4	89.5	113.8	150.7	108.8	96.4	99.1	127.9	102.0	146.2	94.5
DC	87.1	96.3	103.2	116.9	97.7	119.6	94.2	104.7	96.3	106.8	93.3
DF	94.3	127.4	102.5	116.1	103.7	148.5	104.1	95.8	86.1	89.8	82.1

(b) Tall subjects

Position	DA	PM	BB	SA	FF	TD	TT	DP	IS	TB	FE
UB	133.3	105.9	105.2	124.9	115.2	84.5	100.0	104.2	139.6	124.9	140.4
UC	108.2	121.6	101.7	121.8	102.2	83.7	89.0	104.2	102.5	120.1	115.4
UF	85.7	107.4	94.6	95.1	118.0	83.2	90.9	90.4	81.1	98.3	120.0
MB	125.4	82.0	100.6	122.6	113.2	98.6	117.7	105.6	145.2	106.2	125.2
MC	100.0	100.0	100.0	100.0	100.0	100.0	100.0	100.0	100.0	100.0	100.0
MF	93.3	91.8	100.3	107.9	107.5	113.0	86.5	84.8	156.0	104.7	99.8
DB	126.4	78.9	121.2	118.5	121.5	129.5	102.2	112.7	116.5	90.5	123.0
DC	109.5	83.5	101.7	103.2	121.3	132.6	100.4	90.2	112.0	82.6	102.7
DF	99.8	85.3	97.0	99.8	105.3	169.5	90.3	79.1	223.8	81.1	90.6

group showed the smallest CR (97%) at UC position and the largest (104%) at MB position. It is noted that short group tended to show decreased CR as moving forward or downward from MC position and tall group showed the smallest CR at MC position.

4. Discussion and Conclusions

In this study, iEMG and muscle co-contraction were evaluated to determine the optimal riding position of the newly-designed manual standing wheelchair to ride even in standing posture as well as in sitting posture. To investigate how muscle activation was affected by the changes in various riding positions of the manual standing wheelchair, propulsion angle and timing were also analyzed to normalize iEMG data.

In most previous studies on the wheelchair propulsion, the propulsion phase was divided into only push and recovery phases. However, Louis et al.[8] divided the push phase into EP and LP for the more detailed analysis. As a result, they found propulsion time and muscle activation differences between the paraplegic group and the able-bodied group. In the present study, the propulsion cycle was defined as three different

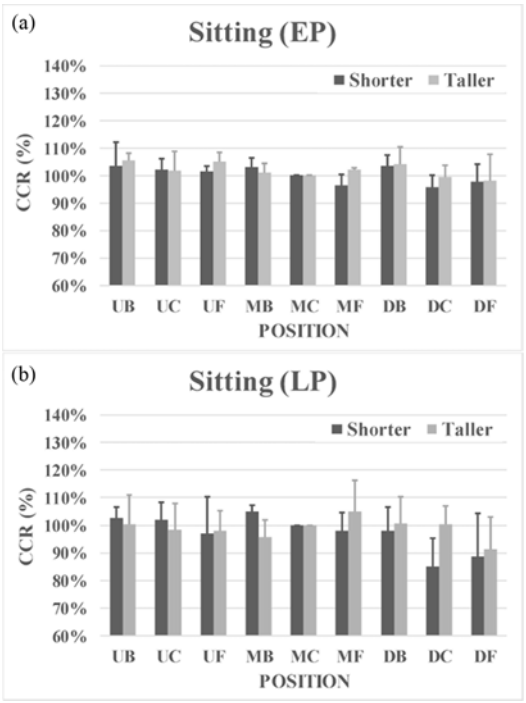

Fig. 8 Muscle co-contraction on propulsion phases in sitting posture for short and tall subject groups, (a) early push time (b) late push time

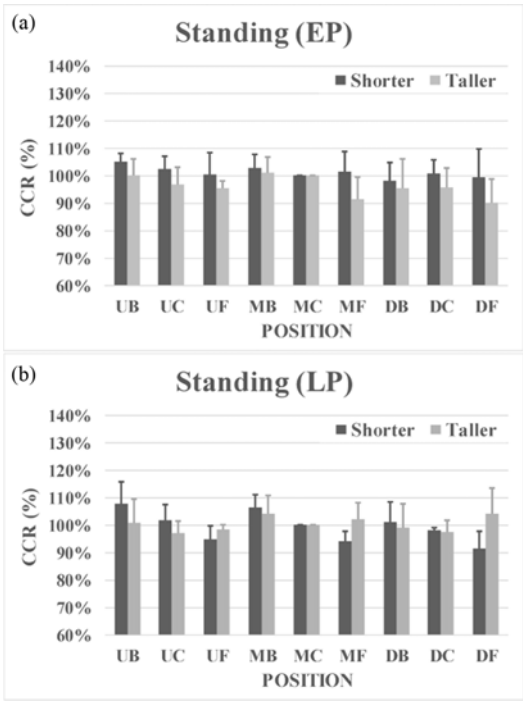

Fig. 9 Muscle co-contraction on propulsion phases in standing posture for short and tall subject groups, (a) early push time (b) late push time

phases: EP, LP and RP. The time before and after when the hand passed the top dead center (TDC) on the hand rim is EP and LP.

4.1 Propulsion angle

Regardless of the subject groups and riding postures, the propulsion angles during EP gradually decreased as the body moved from backward to forward position. On the other hand, during LP, they gradually increased as the body moved from backward to forward positions. The propulsion angles during EP and LP also gradually increased as the body moved from backward to forward position for both groups. The propulsion angles of push phases gradually increased as the body moved from upward to downward positions for both groups. Especially, the propulsion angle during EP was larger than the one during LP only in UC position. As a result, the propulsion angle during EP and LP at UB position was larger than the one at UC position.

These results showed a good similarity with the results of the previous studies. Gorce et al.[17] showed that the propulsion angle decreased as the seat height increased and the body moved forward in typical wheelchair. Korajarvi et al.[18] also showed that the propulsion angles were the largest at the low seat height positions. Other previous studies showed the same results.[5-7] Therefore, the elderly individuals had better sit close to the hand rim to ensure the sufficient propulsion angle in a manual standing wheelchair.

4.2 Propulsion time

Propulsion time during EP, LP, and RP were similar in the short and the tall groups. Propulsion time needs to be compared with the propulsion angle. As showed in table 3, the mean propulsion time for EP, LP, RP were 22.2% (0.29 secs), 18.9% (0.24 secs), and 58.9% (0.76 secs), respectively (Table 3). However, Mean propulsion angles during EP and LP were 48.1° and 72.9°, respectively. It means that angular velocities of the hand rim were 167.4°/s during EP and 305.9°/s during LP, respectively. Angular velocity is almost twice during LP, compare with during EP. Regarding the propulsion time, propulsion efficiency during LP was better than that during EP. Its reason is that the rotational speed of the hand rim greatly decreased during RP.

Louis et al.[8] performed wheelchair riding experiments on the paraplegic group and the able-bodied group and reported that EP time for the paraplegic group became significantly longer than the one for the able-bodied group in spite of no significant difference in push time over a full propulsion cycle. However, this was due to the difference in the experience level and the propulsion pattern between the two groups. The propulsion angle of the experts (paraplegic group) was significantly larger than that of the beginners (able-bodied). In addition, all beginners rode using arcing pattern, whereas the experts mostly used semi-circular or single-looping pattern.[8,18]

4.3 iEMG and muscle co-contraction

In this study, sEMG signals were measured in eleven muscles on the right side of the trunk and the upper extremity to evaluate their activations at nine different positions in sitting and standing postures.

It is very important to investigate muscle activities during wheelchair propulsion, because muscle activity is related to the energy expenditure. Some studies showed that energy expenditures had a linear relationship with IEMG.[9,19] Some researchers performed experimental studies to find the relationship between EMG and seat position and reported that muscle activation increased for lower seat positions during push phases.[8] Masse et al.[7] also investigated propulsion patterns and EMG

for five male paraplegic patients in six different seat positions. They concluded that the backward-low position had the overall lowest IEMG and demonstrated a smoother motion of the elbow and forearm. However, their studies did not consider muscle co-contraction (the simultaneous activation of antagonist muscles around a joint) depending on seat positions.

It has been known in many previous studies that if the seat position was close to the hand rim, muscle activation increased because the propulsion angle and time increased. Increased muscle activation contributes to not only increasing propulsion force, but also stabilizing the propulsion operation. From Gribble's study,[20] muscle co-contraction improved motion accuracy. They assumed that although energetically expensive, co-contraction would be a strategy used by the motor system to facilitate multi-joint arm movement accuracy. They concluded that increases in joint stiffness by muscle co-contraction would have a beneficial effect on limb stability and hence movement accuracy by reducing the perturbing effects of joint interaction torques[20,21] and external forces.[22] In addition, co-activation of antagonist muscles is readily observed early in motor learning, in interactions with unstable mechanical environments and in motor system pathologies.[10,23] In this study, the muscle co-contraction ratio (CR) was larger at positions (upward and backward) distant from the hand rim and smaller at positions (downward and forward) close to the hand rim. These results indicate that increased distance from the hand rim reduces joint stability and increases muscle co-contraction. On the other hand, decreased distance from the hand rim enhances joint stability and decreases muscle co-contraction.

As mentioned, when the propulsion operation is unstable, CR increases and joint stability improved. However, as CR increases, energy consumption increases and muscular fatigue easily occurs because of increased muscle use. Thus, the riding positions with less CR are better with regard to propulsion efficiency.

In another study, co-contraction of the antagonist muscle of the elderly was frequently found than that of the young ones.[11] Since the muscle strength of the elderly decreased, the co-contraction of the antagonist muscle increased in order to perform the stable propulsion motion. Son et al.[12] applied co-contraction of the antagonist muscle and showed that co-contraction ratio (CR) of the elderly decreased significantly in four weeks after upper arm elbow robotic rehabilitation training. This means that as the muscle strength increases, joint stability increases and muscle co-contraction decreases consequently. Therefore, the optimal propulsion position of the manual standing wheelchair can be considered where CR of muscle is relatively small.

In this study, subjects were grouped into two groups based on their height only because arm length is generally proportional to height. As shown in the results, the optimal riding position differs depending on the subjects' heights. Short persons were more likely to be closer to the hand rim than tall group, which is due to the effect of both height and arm length. The optimal position for sitting and standing varied from the subject group. The location of seat and the back support played an important role in wheelchair riding with sitting posture, but the location of the footrest and the back support with standing posture. Therefore, the optimal riding position varies depending on the length of the arm and the length of the upper body in sitting posture, but the leg length also affects the optimal riding position in standing posture. Our study suggested that the optimal position in standing posture for the short group was closer to the hand rim than that in sitting posture, but the optimal position in sitting posture for the tall group was farther away from the hand rim than that in the standing posture.

Standing wheelchairs have been developed for the normal elderly who have higher risks of injury due to the improper wheelchair propulsion. Therefore, this study showed the method to determine the optimal riding positions to reduce the risks of injury for the novice with the efficient propulsion. In our previous study regarding the propulsion energy expenditure during the manual standing wheelchair propulsion,[3] the optimal position with the smallest propulsion energy expenditure was located near downward-forward direction. The optimal position of the short subject group was the closest position to the hand rim and the optimal position of the tall subject group was slightly away from the hand rim, but closer to MC position toward the hand rim. In this study, the muscle co-contraction ratio was higher at positions (upward and backward directions) distant from the hand rim and lower at positions (downward and forward directions) close to the hand rim. These results indicate that increased distance from the hand rim reduces joint stability and increases muscle co-contraction. On the other hand, decreased distance from the hand rim enhances joint stability and decreases muscle co-contraction. The evaluation results of energy expenditure and muscle co-contraction showed a good similarity. We believe that these methods and results will be helpful in assessing the adequacy of the riding position of various types of wheelchair.

4.4 Limitations of the study

The measured data of this study were obtained using a wheelchair dynamometer; therefore, the results could be different with a level surface. However, Koontz et al.[24] reported that there was a high positive correlation between the biomechanical parameters measured from a level surface and a dynamometer. Therefore, they concluded that both conditions have similar propulsion mechanisms.

ACKNOWLEDGEMENT

This research was supported by The Leading Human Resource Training Program of Regional Neo industry (No.2016H1D5A1909760) and The Bio & Medical Technology Development Program (No. 2017 M3A9E2063270) through the National Research Foundation of Korea (NRF) funded by the Ministry of Science, ICT.

REFERENCES

1. Kaye, H. S., Kang, T., and LaPlante, M. P., “Mobility Device Use in the United States,” National Institute on Disability and Rehabilitation Research, US Department of Education Washington, DC, 2000.

2. Subbarao, J. V., Klopfstein, J., and Turpin, R., “Prevalence and Impact of Wrist and Shoulder Pain in Patients with Spinal Cord Injury,” The Journal of Spinal Cord Medicine, Vol. 18, No. 1, pp. 9-13, 1995.

3. Ryu, J., Son, J., Jo, M., Choi, E., Ahn, S., Kim, S., and Kim, Y.-H., “Optimal Seat and Footrest Positions of Manual Standing Wheelchair,”

Int. J. Precis. Eng. Manuf., Vol. 18, No. 6, pp. 879-885, 2017.

4. Brubaker, C., "Wheelchair Prescription: An Analysis of Factors that Affect Mobility and Performance," Journal of Rehabilitation Research and Development, Vol. 23, No. 4, pp. 19-26, 1986.
5. Van der Woude, L., Veeger, D.-J., Rozendal, R., and Sargeant, T., "Seat Height in Handrim Wheelchair Propulsion," Journal of Rehabilitation Research and Development, Vol. 26, No. 4, pp. 31-50, 1989.
6. Boninger, M. L., Souza, A. L., Cooper, R. A., Fitzgerald, S. G., Koontz, A. M., and Fay, B. T., "Propulsion Patterns and Pushrim Biomechanics in Manual Wheelchair Propulsion," Archives of Physical Medicine and Rehabilitation, Vol. 83, No. 5, pp. 718-723, 2002.
7. Masse, L., Lamontagne, M., and O'riain, M., "Biomechanical Analysis of Wheelchair Propulsion for Various Seating Positions," Journal of Rehabilitation Research and Development, Vol. 29, No. 3, pp. 12-28, 1992.
8. Louis, N. and Gorce, P., "Surface Electromyography Activity of Upper Limb Muscle during Wheelchair Propulsion: Influence of Wheelchair Configuration," Clinical Biomechanics, Vol. 25, No. 9, pp. 879-885, 2010.
9. Henriksson, J. and Bonde-Petersen, F., "Integrated Electromyography of Quadriceps Femoris Muscle at Different Exercise Intensities," Journal of Applied Physiology, Vol. 36, No. 2, pp. 218-220, 1974.
10. Darainy, M. and Ostry, D. J., "Muscle Cocontraction Following Dynamics Learning," Experimental Brain Research, Vol. 190, No. 2, pp. 153-163, 2008.
11. Häkkinen, K., Newton, R. U., Gordon, S. E., McCormick, M., Volek, J. S., et al., "Changes in Muscle Morphology, Electromyographic Activity, and Force Production Characteristics during Progressive Strength Training in Young and Older Men," The Journals of Gerontology Series A: Biological Sciences and Medical Sciences, Vol. 53, No. 6, pp. B415-B423, 1998.
12. Son, J., Ryu, J., Ahn, S., Kim, E. J., Lee, J. A., and Kim, Y., "Effects of 4-Week Intensive Active-Resistive Training with an EMG-Based Exoskeleton Robot ON Muscle Strength in Older People: A Pilot Study," BioMed Research International, Vol. 2016, Article ID: 1256958, 2016.
13. Arva, J., Paleg, G., Lange, M., Lieberman, J., Schmeler, M., Dicianno, B., Babinec, M., and Rosen, L., "Resna Position on the Application of Wheelchair Standing Devices," Assistive Technology, Vol. 21, No. 3, pp. 161-168, 2009.
14. Dunn, R. B., Walter, J. S., Lucero, Y., Weaver, F., Langbein, E., et al, "Follow-Up Assessment of Standing Mobility Device Users," Assistive Technology, Vol. 10, No. 2, pp. 84-93, 1998.
15. Karmarkar, A. M., Dicianno, B. E., Graham, J. E., Cooper, R., Kelleher, A., and Cooper, R.A., "Factors Associated with Provision of Wheelchairs in Older Adults," Assistive Technology, Vol. 24, No. 3, pp. 155-167, 2012.
16. Requejo, P. S., Furumasu, J., and Mulroy, S. J., "Evidence-Based Strategies for Preserving Mobility for Elderly and Aging Manual Wheelchair Users," Topics in Geriatric Rehabilitation, Vol. 31, No. 1, pp. 26, 2015.
17. Gorce, P. and Louis, N., "Wheelchair Propulsion Kinematics in Beginners and Expert Users: Influence of Wheelchair Settings," Clinical Biomechanics, Vol. 27, No. 1, pp. 7-15, 2012.
18. Kotajarvi, B. R., Sabick, M. B., An, K.-N., and Zhao, K. D., "The Effect of Seat Position on Wheelchair Propulsion Biomechanics," Journal of Rehabilitation Research and Development, Vol. 41, No. 3B, pp. 403-414, 2004.
19. Bigland-Ritchie, B. and Woods, J. J., "Integrated Electromyogram and Oxygen Uptake during Positive and Negative Work," The Journal of Physiology, Vol. 260, No. 2, pp. 267-277, 1976.
20. Gribble, P. L., Mullin, L. I., Cothros, N., and Mattar, A., "Role of Cocontraction in Arm Movement Accuracy," Journal of Neurophysiology, Vol. 89, No. 5, pp. 2396-2405, 2003.
21. Koshland, G. F., Galloway, J. C., and Nevoret-Bell, C. J., "Control of the Wrist in Three-Joint Arm Movements to Multiple Directions in the Horizontal Plane," Journal of Neurophysiology, Vol. 83, No. 5, pp. 3188-3195, 2000.
22. Gomi, H. and Osu, R., "Task-Dependent Viscoelasticity of Human Multijoint Arm and Its Spatial Characteristics for Interaction with Environments," Journal of Neuroscience, Vol. 18, No. 21, pp. 8965-8978, 1998.
23. Firouzimehr, Z., "The Role of Muscle Cocontraction in Motor Learning," M.Sc. Thesis, McGill University, 2011.
24. Koontz, A. M., Worobey, L. A., Rice, I. M., Collinger, J. L., and Boninger, M. L., "Comparison between Overground and Dynamometer Manual Wheelchair Propulsion," Journal of Applied Biomechanics, Vol. 28, No. 4, pp. 412-419, 2012.